Quasiperiodic and Chaotic Dynamics in Bose-Einstein Condensates in Periodic Lattices and Superlattices

Martijn van Noort
m.vannoort@imperial.ac.uk
Department of Mathematics
Imperial College, London SW7 2AZ, UK

Mason A. Porter*
mason@caltech.edu
Department of Physics and Center for the Physics of Information
California Institute of Technology, Pasadena, CA 91125

Yingfei Yi
yi@math.gatech.edu
Center for Dynamical Systems and Nonlinear Studies, School of Mathematics
Georgia Institute of Technology, Atlanta, GA 30332

Shui-Nee Chow
chow@math.gatech.edu
Center for Dynamical Systems and Nonlinear Studies, School of Mathematics
Georgia Institute of Technology, Atlanta, GA 30332

July 23, 2005

Abstract

We employ KAM theory to rigorously investigate the transition between quasiperiodic and chaotic dynamics in cigar-shaped Bose-Einstein condensates (BEC) in periodic lattices and superlattices. Toward this end, we apply

*Corresponding author

a coherent structure ansatz to the Gross-Pitaevskii equation to obtain a parametrically forced Duffing equation describing the spatial dynamics of the condensate. For shallow-well, intermediate-well, and deep-well potentials, we find KAM tori and Aubry-Mather sets to prove that one obtains mostly quasiperiodic dynamics for condensate wave functions of sufficiently large amplitude, where the minimal amplitude depends on the experimentally adjustable BEC parameters. We show that this threshold scales with the square root of the inverse of the scattering length, whereas the rotation number of tori above this threshold is proportional to the amplitude. As a consequence, one obtains the same dynamical picture for lattices of all depths, as an increase in its amplitude essentially only affects scaling in phase space. Our approach is applicable to periodic superlattices with an arbitrary number of rationally dependent wave numbers.

MSC: 37J40, 70H99, 37N20

PACS: 05.45.-a, 03.75.Lm, 05.30.Jp, 05.45.Ac, 03.75.Nt

Keywords: Hamiltonian dynamics, Bose-Einstein condensates, KAM theory, Aubry-Mather theory

1 Introduction

Bose-Einstein condensates (BECs) have generated considerable excitement in the physics community both because their study allows one to explore new regimes of fundamental physics and because of their eventual engineering applications. They constitute a macroscopic quantum phenomenon, and their analysis has already lead to an increased understanding of phenomena such as superfluidity and superconductivity. Of particular interest are BECs in optical lattices (periodic potentials), which have already been used to study Josephson effects,[1] squeezed states,[37] Landau-Zener tunneling and Bloch oscillations,[31] and the transition between superfluidity and Mott insulation.[9,18,44] With each lattice site occupied by one alkali atom in its ground state, BECs in periodic potentials also show promise as a register in a quantum computer.[43,46]

In the present paper, we generalize recent work on near-autonomous dynamics in BECs[40,41] to study chaotic behavior in BECs in periodic lattices, which can have shallow, intermediate, or deep wells. We present our methodology and results in section 1.1. In section 2, we discuss the physics of BECs and use a coherent structure ansatz to derive a parametrically forced Duffing oscillator describing the spatial dynamics of the condensate. The transition in phase space from quasiperiodic dynamics to chaotic dynamics of parametrically forced Duffing oscillators is rigorously investigated in section 3. Sections 3.1 and 3.2 then describe applications to BECs in periodic lattices and periodic superlattices, respectively. The KAM theorem used in this analysis is proven in section 4.

1.1 Methodology and results

The spatial dynamics of standing wave solutions in BECs in periodic optical lattices can be described by a parametrically forced Duffing equation, where the periodic forcing is given by an external potential due to the lattice.[7,40,41] This constitutes a $1\frac{1}{2}$ degree of freedom Hamiltonian system, and we employ KAM theory and Aubry-Mather theory to study its quasi-periodic dynamics and to find the phase space boundaries between quasiperiodic and chaotic behavior. Previous studies concerning KAM transitions in BECs took a heuristic approach and considered only near-autonomous situations.[40,41] The approach of this paper, however, is especially versatile in that shallow, deep, and intermediate lattice wells can all be considered using the same mathematical framework. That is, we consider the near-autonomous and far-from-autonomous settings simultaneously.

Theorem 5 proves that for any (analytic) external periodic potential, any negative scattering length, and any chemical potential, one obtains mostly 2-quasiperiodic dynamics for condensate wave functions of sufficiently large amplitude, where the minimal amplitude depends on the experimentally adjustable BEC parameters. In particular, the threshold amplitude is proportional to the reciprocal of the square root of the scattering length. Any 2-quasiperiodic wave function above the threshold has one fixed frequency and one proportional to its amplitude. We also demonstrate numerically that one obtains the same dynamical picture for lattices of all depths, as an increase in lattice amplitude essentially only affects scaling in phase space. These numerical results support the theoretically predicted scaling of the threshold amplitude. Our theorem applies to periodic superlattices with an arbitrary number of rationally dependent wave numbers.

The system that we investigate is given by a Hamiltonian of the form $H(R,S,\xi) = \frac{1}{2}S^2 + U(R,\xi)$, where $|R|$ is the amplitude of the wave function, R and S are conjugate variables, $\xi \in \mathbb{R}/\mathbb{Z}$ with $\xi' = 1$, and U is a polynomial in R and 1-periodic in ξ. We also consider its Poincaré map, defined to be the return map on the section $\xi = 0$.

One can show that such systems have invariant tori sufficiently far from the origin $(R,S) = (0,0)$, even when they are far from autonomous (that is, even when H is a large perturbation of an ξ-independent system). In the present case, this implies the existence of invariant tori for any optical lattice depth. The key condition is that $U(R,\xi)/R^2 \to +\infty$ as $R \to \pm\infty$, as this guarantees that the set of frequencies corresponding to rotation around the origin is unbounded; indeed, the frequency goes to infinity with the distance to the origin. The first result of this type can be found in the equivalent context of adiabatic theory.[3] Another strand goes back to the question of boundedness of solutions (which is implied by the existence of invariant tori in this low-dimensional situation).[24] These qualitative results have been extended to more general mathematical settings.[14,23,25,33,34,48]

A typical system of this type exhibits a phase space divided into two clearly distinct regions. See figures 1 – 3, which show numerical experiments in the present

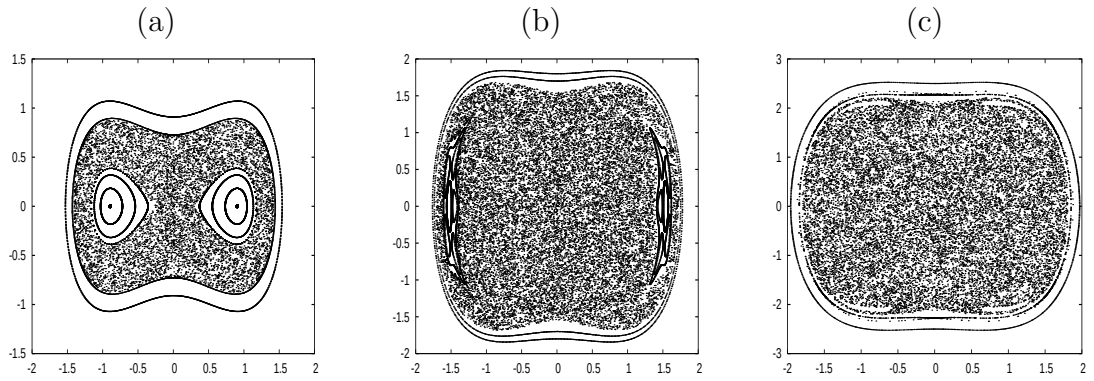

Figure 1: Phase portraits of the Poincaré map P for the example of section 3.1, with horizontal axis R and vertical axis S. In this case the Hamiltonian is of the form $H = \frac{1}{2}S^2 - \frac{1}{2}(1+V_1\cos(\xi))R^2 + \frac{1}{4}R^4$. Observe the invariant curves for large R in these figures. Generically, the invariant manifolds of the central saddle point intersect transversally, creating a homoclinic tangle and thereby implying the existence of horseshoes of measure zero. By conjecture, the closure of these horseshoes is a "chaotic sea" of positive measure, corresponding to the dots in the figures. As the size of the perturbation V_1 is increased to $+\infty$, the size of each of the remaining integrable islands vanishes, but their total measure remains $O(1)$. The values of V_1 are (a) $V_1 = 0.1$, (b) $V_1 = 0.5$, and (c) $V_1 = 1$.

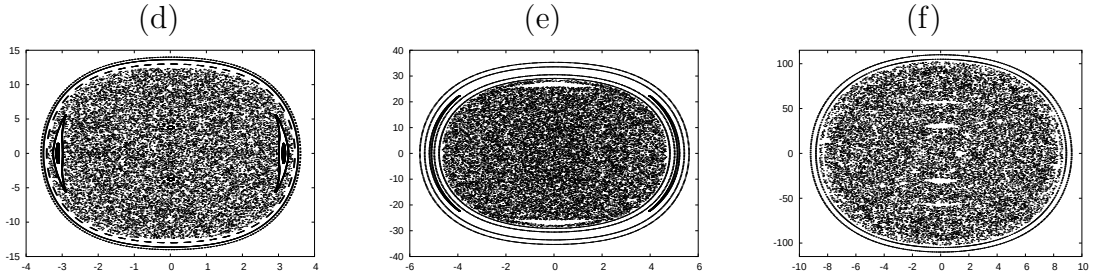

Figure 2: Continuation of figure 1. Phase portraits of the Poincaré map P at (d) $V_1 = 10$, (e) $V_1 = 25$, and (f) $V_1 = 100$.

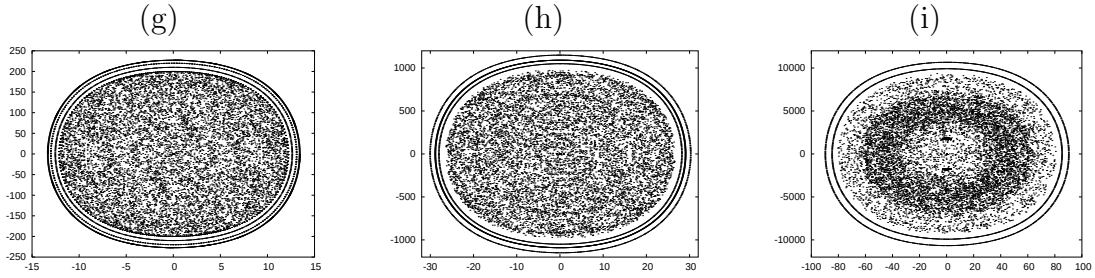

Figure 3: Continuation of figure 2. Phase portraits of the Poincaré map P at (g) $V_1 = 200$, (h) $V_1 = 1000$, and (i) $V_1 = 10000$.

setting. One region, bounded away from the origin, consists largely of invariant tori, with small layers of chaotic dynamics between them. Indeed, one can show that the measure of these layers vanishes exponentially fast as the distance to the origin goes to infinity.[6,35] The other region has mainly chaotic dynamics.

In this paper, we employ a quantitative existence result[11] to obtain bounds on the location and frequencies of invariant tori and consequently on the transition between regular and chaotic motion.

2 Physical Background and Coherent Structures

At low temperatures, particles in a dilute boson gas can reside in the same quantum (ground) state, forming a Bose-Einstein condensate (BEC).[12] This was first observed experimentally in 1995 with vapors of rubidium and sodium.[2,13] In these experiments, atoms were confined in magnetic traps, evaporatively cooled to temperatures on the order of fractions of microkelvins, left to expand by switching off the confining trap, and subsequently imaged with optical methods.[12] A sharp peak in the velocity distribution was observed below a critical temperature, indicating that condensation had occurred. BECs are inhomogeneous, allowing condensation to be observed in both momentum and position space. The number of condensed atoms N ranges from several thousand to several million.

A BEC has two characteristic length scales: the harmonic oscillator length $a_{ho} = \sqrt{\hbar/[m\omega_{ho}]}$ (which is about a few microns), where $\omega_{ho} = (\omega_x\omega_y\omega_z)^{1/3}$ is the geometric mean of the trapping frequencies, and the mean healing length $\chi = 1/\sqrt{8\pi|a|\bar{n}}$, where $\bar{n}$ is the mean density and a, the (two-body) s-wave scattering length, is determined by the atomic species of the condensate. Interactions between atoms are repulsive when $a > 0$ and attractive when $a < 0$. For a dilute ideal gas, $a \approx 0$. The length scales in BECs should be contrasted with those in systems like superfluid helium, in which the effects of inhomogeneity occur on a microscopic scale fixed by the interatomic distance.[12]

When considering only two-body interactions, the BEC wave function ("order parameter") $\psi(x,t)$ satisfies the Gross-Pitaevskii (GP) equation,

$$i\hbar\psi_t = -[\hbar^2/(2m)]\psi_{xx} + g|\psi|^2\psi + V(x)\psi\,, \tag{1}$$

where $|\psi|^2$ is the number density, $V(x)$ is an external potential, $g = [4\pi\hbar^2 a/m][1 + \mathcal{O}(\zeta^2)]$, and $\zeta = \sqrt{|\psi|^2|a|^3}$ is the dilute gas parameter.[12] BECs are modeled in the quasi-one-dimensional (quasi-1D) regime when the transverse dimensions of the condensate are on the order of its healing length and its longitudinal dimension is much larger than its transverse ones.[7] In the quasi-1D regime, one employs the 1D limit of a 3D mean-field theory rather than a true 1D mean-field theory, which would be appropriate were the transverse dimension on the order of the atomic interaction length or the atomic size. Because the scattering length a can be adjusted using

a magnetic field in the vicinity of a Feshbach resonance,[16] the contribution of the nonlinearity in (1) is tunable.

Potentials $V(x)$ of interest include harmonic traps, periodic lattices and superlattices (i.e., optical lattices with two or more wave numbers), and periodically perturbed harmonic traps. The existence of quasi-1D cylindrical ("cigar-shaped") BECs motivates the study of periodic potentials without a confining trap along the dimension of the periodic lattice.[27] Experimentalists use a weak harmonic trap on top of the periodic lattice or superlattice to prevent the particles from spilling out. To achieve condensation, the lattice is typically turned on after the trap. If one wishes to include the trap in theoretical analyses, $V(x)$ is modeled by

$$V(x) = V_1 \cos(\kappa_1 x) + V_2 \cos(\kappa_2 x) + V_h x^2 \,, \tag{2}$$

where κ_1 is the primary lattice wave number, $\kappa_2 > \kappa_1$ is the secondary lattice wave number, V_1 and V_2 are the associated lattice amplitudes, and V_h represents the magnitude of the harmonic trap. (Note that V_1, V_2, V_h, κ_1, and κ_2 can all be tuned experimentally.) When $V_h \ll V_1\,, V_2$, the potential is dominated by its periodic contributions for many periods. BECs in optical lattices with up to 200 wells have been created experimentally.[38]

In this work, we let $V_h = 0$ and focus on periodic lattices and superlattices. Spatially periodic potentials have been employed in experimental studies of BECs[1,19] and have also been studied theoretically.[7,8,28,47] In recent experiments, BECs were created in superlattices with $\kappa_2 = 3\kappa_1$.[39] However, there has thus far been almost no theoretical research on BECs in superlattices.[15,17,26,42]

As mentioned in section 1.1 and proven below, we obtain bounds on the location and frequencies of invariant tori and consequently on the transition between regular and chaotic motion. The importance of investigating the onset of chaotic dynamics in BECs has been noted previously.[8,10,40,41,45] In the present framework, the presence of chaos reflects an irregular spatial profile $R(x)$ (where $|R(x)| = |\psi(x,t)|$ is the amplitude of the BEC wave function) and invariant tori correspond to regular spatial profiles.

Remark 1 : When the optical lattice has deep wells (large $|V_1|$ or $|V_2|$), one can also obtain an analytical description of BECs in terms of Wannier wave functions using the so-called "tight-binding approximation".[30] In this regime, the BEC dynamics are described using what is known as the Bose-Hubbard model, which is derived by expanding the field operator in a Wannier basis of localized wave functions at each lattice site.

Coherent structures solutions are described with the ansatz

$$\psi(x,t) = R(x) \exp\left(i\left[\theta(x) - \mu t\right]\right) \,, \tag{3}$$

where $R \in \mathbb{R}$ gives the amplitude dynamics of the wave function $[|R(x)| = |\psi(x,t)|]$, $\theta(x)$ gives the phase dynamics, and the "chemical potential" μ, defined as the energy

it takes to add one more particle to the system, is proportional to the number of atoms trapped in the condensate. When the (temporally periodic) coherent structure (3) is also spatially periodic, it is called a *modulated amplitude wave* (MAW).[41] The orbital stability of MAWs for the cubic NLS with elliptic potentials has been studied by Bronski and co-authors.[7] To obtain stability information about sinusoidal potentials, one takes the limit as the elliptic modulus approaches zero.

Inserting (3) into the NLS (1) and equating real and imaginary parts, one obtains

$$\hbar\mu R(x) = -\frac{\hbar^2}{2m}R''(x) + \left[\frac{\hbar^2}{2m}\left[\theta'(x)\right]^2 + gR^2(x) + V(x)\right]R(x)\,, \tag{4}$$
$$0 = \frac{\hbar^2}{2m}\left[2\theta'(x)R'(x) + \theta''(x)R(x)\right]\,,$$

which gives the following nonlinear ordinary differential equation:

$$R'' = \frac{c^2}{R^3} - \frac{2m\mu R}{\hbar} + \frac{2mg}{\hbar^2}R^3 + \frac{2m}{\hbar^2}V(x)R\,. \tag{5}$$

The parameter c is defined via the relation

$$\theta'(x) = \frac{c}{R^2(x)}\,, \tag{6}$$

which plays the role of conservation of "angular momentum," as discussed by Bronski and coauthors.[7] Constant phase solutions (i.e., standing waves) constitute an important special case and satisfy $c = 0$. In the rest of the paper, we consider only standing waves, so that

$$R'' = -\frac{2m\mu R}{\hbar} + \frac{2mg}{\hbar^2}R^3 + \frac{2m}{\hbar^2}V(x)R\,. \tag{7}$$

Remark 2 : The case $c \neq 0$ describing coherent structures with nonzero angular momentum exhibits the same qualitative behavior for large R as do the standing waves. Furthermore, we expect the estimates we prove below to hold in this more general case, as the additional term in (5) is very small in this regime. However, this situation is more difficult technically, so we omit it.

Remark 3 : When $V(x) \equiv 0$, the dynamical system (7) is the autonomous, integrable Duffing oscillator. Its qualitative dynamics in the physically relevant situation of bounded $|R|$ are illustrated in figure 4. The methodology developed in the present paper can handle attractive BECs ($g < 0$) with either $\mu < 0$ or $\mu > 0$ but not repulsive BECs, as equation (7) has unbounded solutions when $g > 0$.

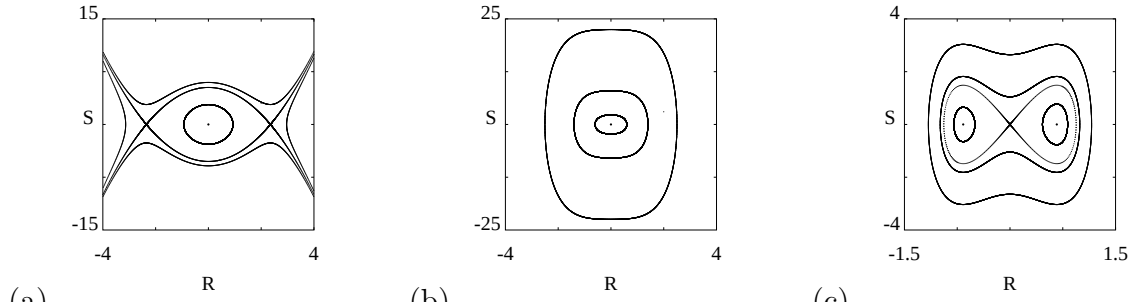

(a) (b) (c)

Figure 4: Phase portraits of coherent structures in BECs with no external potential. The signs of μ and g determine the dynamics of (7). (a) Repulsive BEC with $\mu > 0$. Orbits inside the separatrix have bounded amplitude $|R(x)|$. The period of such orbits increases as one approaches the separatrix. In this case, the dynamical system can be rescaled so that $R'' = -R + R^3$. (b) Attractive BEC with $\mu > 0$. The dynamical system can be rescaled so that $R'' = -R - R^3$. (c) Attractive BEC with $\mu < 0$. Here there are two separatrices, each of which encloses periodic orbits satisfying $R \neq 0$. The dynamical system can be rescaled so that $R'' = R - R^3$.

3 Main Result

This section states the main theorem of this paper, which concerns the existence of quasiperiodic dynamics in a class of systems of the form (7), including the cases of periodic lattices and superlattices. Applications to these cases are subsequently given in two subsections.

The equation of motion (7) describes a $1\frac{1}{2}$ degree of freedom Hamiltonian system with periodic forcing. We will allow arbitrary analytic periodic potential functions V. We first rescale the period of the forcing to 1. Introduce the phase variable $\xi = T^{-1}x \,(\mathrm{mod}\, 1)$, where $T > 0$ is the minimal period of V. Letting $'$ denote derivation with respect to ξ, we define $S = R'$, and

$$z_2(\xi) = T^2\left(\frac{m\mu}{\hbar} - \frac{m}{\hbar^2}V(x)\right), \quad z_4 = -T^2\frac{mg}{2\hbar^2}, \quad U(R,\xi) = z_2(\xi)R^2 + z_4R^4.$$

This gives the suspended dynamical system

$$\begin{aligned} R' &= S\,, \\ S' &= -\frac{\partial U}{\partial R}(R,\xi)\,, \\ \xi' &= 1\,, \end{aligned} \tag{8}$$

with Hamiltonian

$$H(R,S,\xi) = \frac{1}{2}S^2 + U(R,\xi)\,. \tag{9}$$

Remark 4 : As $z_4 > 0$, the potential function U is a well; that is, $U \to +\infty$ as $R \to \pm\infty$ for all ξ. It is even in R, which has important ramifications for the sizes of the perturbations in our subsequent analysis. (See, for example, lemma 14 below, where the leading term in the nonintegrable parts F_1 and F_2 would have been order one instead of going to zero as $R \to +\infty$, were it not for this symmetry.)

We introduce action-angle coordinates as follows. (The details are in section 4.) Let $H_0(R,S) = \frac{1}{2}S^2 + z_4R^4$. For $h > 0$, define the action $I = I(h)$ to be the area in the (R,S)-plane enclosed by the curve $H_0(R,S) = h$. Let the angle $\phi = \phi(R,S) \in \mathbb{R}/\mathbb{Z}$ be such that the transformation $(R,S) \mapsto (\phi, I)$ is symplectic. This defines ϕ uniquely if we set $\phi(0,S) \equiv 0$ for $S > 0$.

In action-angle coordinates, the Hamiltonian takes the form $K(\phi, I, \xi) = K_0(I) + K_1(\phi, I, \xi)$, where $K_0(I) = H_0(R,S)$. We consider K as a perturbation of K_0. For any $I_0 > 0$, the unperturbed system K_0 has an invariant torus $I = I_0$ with frequency $\omega = K_0'(I_0)$ in ϕ. We say that this frequency is of *constant type* with parameter $\gamma > 0$ if

$$\left|\omega - \frac{p}{q}\right| \geq \gamma q^{-2} \quad \text{for all} \quad \frac{p}{q} \in \mathbb{Q}\,. \tag{10}$$

This is a special type of Diophantine condition.[20,21]

For a function f defined on a set $\mathcal{D}$, we define $||f||_{\mathcal{D}} = \sup_{\mathcal{D}} |f|$. If f is vector-valued, then $||f||_{\mathcal{D}}$ is the maximum of the norms of the components. For $d > 0$, let $\bar{\mathcal{D}}(d) = \{\xi \in \mathbb{C}/\mathbb{Z} : |\mathrm{Im}(\xi)| \leq 2d\}$.

With the additional notation $\eta = 18\gamma$, $M = z_4 I_0$, $c = 126/25 = 5.04$, and $b_1 = \int_0^1 (1-u^4)^{1/2}\,\mathrm{d}u = 0.874019\ldots$, the main result of this paper can now be stated as follows.

Theorem 5 *The Hamiltonian K has an invariant torus with frequency $\omega = K_0'(I_0)$ in ϕ if there exist ν, γ, $d > 0$ and $b_2 > 0$ with $0 \leq \nu \leq \frac{1}{9}2^{-7/3}$ and $0 < \gamma \leq \frac{49}{72}$, such that ω is of constant type with parameter γ and the following conditions hold:*

$$A\left(1 + \frac{3\log B}{\log M}\right) \leq 2^{-4/3} b_1^{-4/3} \log(2) \tag{11}$$

$$1 < M \tag{12}$$

$$L \leq \frac{47}{200} \tag{13}$$

$$b_2 \leq 18(1 + 24b_1(\eta + 2d))(1+L)^{2/3}(1-L)^{1/3}\log(M) \tag{14}$$

$$2 \leq BM^{1/3} \tag{15}$$

$$||z_2||_{\bar{\mathcal{D}}(d)} \leq \delta \frac{M^{2/3}}{\log^2(M)}, \tag{16}$$

where

$$
\begin{aligned}
L &= 2^{4/3}\cdot 3b_1^{4/3}\eta M^{-1/3}+\frac{2b_2 d}{\log(M)}\\
A &= \frac{1+4(\eta+2d)}{d}\max\left\{\frac{2\eta}{3}M^{-1/3}\log(M)+\left(\frac{2^{2/3}}{9}+\frac{7\nu}{2}\right)db_1^{-4/3}b_2+\right.\\
&\quad \left.\frac{2^{-1/3}}{27}b_1^{-4/3}(1-L)^{-5/3}L^2\log(M), 2M^{-1/3}\log(M)+\frac{3\nu}{2}db_1^{-4/3}b_2\right\}\\
B &= 2^{-13/3}3^3 7^8 c^{-1}db_1^{-4/3}b_2\eta^{-6}\left(\frac{1}{\log(M)}+\frac{2^{-7/3}}{3}b_1^{-4/3}b_2\frac{M^{1/3}}{\log^2(M)}\right)\\
\delta &= \frac{2^{-1/3}}{3}\nu d b_2^2 b_1^{-5/3}(1+L)^{-2/3}(1+24b_1(\eta+2d))^{-3}.
\end{aligned}
$$

The torus lies in the region given by $|I-I_0|\le b_2 I_0(\log(z_4 I_0))^{-1}(\frac{11}{19}d+\rho)$.

Remark 6 : Conditions (11) – (15) are satisfied for M sufficiently large, while (16) is a restriction on z_2 and hence on V. The theorem implies that $||z_2||_{\bar{D}(d)}$ can be taken roughly proportional to $z_4^{2/3}I_0^{2/3}$. Equation (23) below shows that $z_4^{-1/6}I_0^{1/3}$ is proportional to the maximal R coordinate $R_{\max}$ on the torus $H_0(R,S)=K_0(I_0)$, so $||z_2||_{\bar{D}(d)}$ is roughly proportional to $z_4 R_{\max}^2$. This fits with the numerically computed phase portraits in figures 1 – 3.

In terms of physical parameters, this implies that for an attractive BEC with given scattering length $a<0$ and chemical potential μ loaded into an arbitrary periodic lattice of amplitude $||V||$ (with any number of wave numbers), the wave function's spatial component $R(x)$ is quasiperiodic with two frequencies (rather than chaotic) if its maximum $R_{\max}$ is large enough, its frequencies satisfy the Diophantine condition (10), and the amplitude $||V||$ of the lattice potential is sufficiently small. The lower bound on $R_{\max}$ scales as $\kappa/\sqrt{|a|}$, where $\kappa=2\pi/T$ is the lattice wave number, whereas the upper bound on $||V||$ scales as $aR_{\max}^2$. All frequency ratios that are algebraic numbers of index 2 satisfy the Diophantine condition (for some $\gamma>0$).

Remark 7 : The conditions of the theorem imply that M should be larger than roughly 10^6. Indeed, from $A\ge 8\cdot 2M^{-1/3}\log(M)$ and $BM^{1/3}\ge 2$, it follows that $A(1+3\log(B)/\log(M))\ge 48M^{-1/3}\log(2)$. Hence condition (11) implies that $M\ge 2^{16}3^3b_1^4\approx 10^6$.

As an illustration, we choose M and the parameters b_2, γ, d, ν based on a numerical experiment where we evaluate the conditions of the theorem on a Cartesian grid of $360\times 180\times 120\times 120\times 20$ points in the cube $[10^6,10^{18}]\times[10^{-6},1]\times[10^{-3},10]\times[10^{-3},10]\times[10^{-3},\frac{1}{9}2^{-7/3}]$ in (M,b_2,γ,d,ν) space, taking a logarithmic scale in the first four components and a linear scale in the last. For each M, we compute the largest value of the coefficient δ over all grid points where all the conditions hold in

order to obtain a good choice of parameter values. Figure 5 shows for a range of M the largest δ one can obtain.

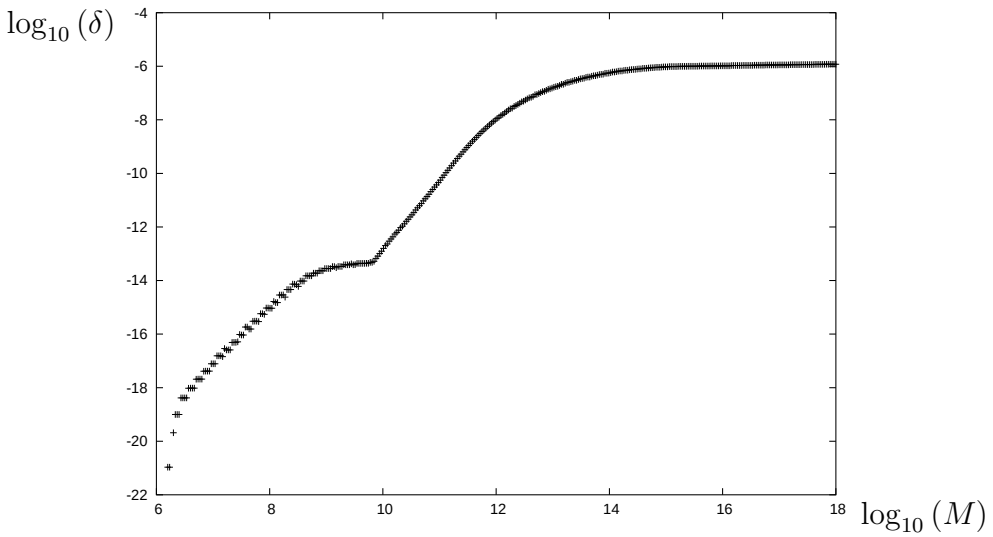

Figure 5: Log-log plot of M against the largest value of δ found by a numerical computation.

Corollary 8 *If K has an invariant torus with frequency $K_0'(I_0)$ then the return map of K on the surface of section $\xi = 0$ has an Aubry-Mather set with rotation number ω for any $\omega > K_0'(I_0)$.*

The corollary follows immediately from Aubry-Mather theory[4, 29, 32] and the monotonicity of K_0'. It implies that the region outside the innermost invariant torus is very regular: it consists largely of invariant tori that are either continuous or of Cantor-type. By contrast, the region on the inside exhibits chaotic dynamics, as can be seen in figures 1 – 3. In the near-autonomous setting (i.e., for small-amplitude V), the figures show large domains of integrable dynamics in the interior region. As the amplitude of V goes to infinity, the sizes of these islands vanish, but their number increases reciprocally, so that an integrable set of measure $O(1)$ remains.[36]

In the next two sections, we consider potential functions $V(x)$ with one and two wave numbers. The former case describes BECs in periodic lattices,[7, 8, 28, 40, 41] and the latter case, which is still sparsely studied even though it is now experimentally accessible, describes BECs in periodic superlattices.[15, 17, 26, 39, 42]

3.1 Example 1: BECs in Periodic Lattices

Optical lattice potentials are created experimentally as interference patterns of counter-propagating laser beams. In the periodic case, the external potential is typically taken to be sinusoidal,

$$V(x) = -V_1 \cos(\kappa x)\,, \tag{17}$$

where $\kappa = 2\pi/T$ is the lattice wave number.

We write equation (7) in the form

$$\begin{aligned} R' &= S\,, \\ S' &= -\alpha_1 R + \alpha_3 R^3 + V_1 R\cos(\kappa x)\,, \\ x' &= 1\,, \end{aligned} \tag{18}$$

where $\alpha_1 \propto \mu$, $\alpha_3 \propto g$, and $'$ denotes derivation with respect to x. The parameters $V_1\,, \alpha_1\,, \alpha_3 \in \mathbb{R}$, and $\kappa > 0$ can all be adjusted experimentally. The phase variables are $(R, S) \in \mathbb{R}^2$ and $x \in \mathbb{R}/(2\pi\kappa^{-1}\mathbb{Z})$. The associated Poincaré map P, which is defined to be the first return map on the section $x = 0$, corresponds to the flow over $2\pi\kappa^{-1}$.

Equation (18) has two reversible symmetries:

$$(R, S, x) \mapsto (-R, S, -x)\,, \quad (R, S, x) \mapsto (R, -S, -x).$$

The map P is thus reversible under reflection in both coordinate axes,

$$R_j \circ P \circ R_j = P^{-1}\,, \quad j = 1, 2\,,$$

where R_1 and R_2 are the reflections with respect to the axes.

Additionally, (18) is invariant under two rescalings:

$$(R, S, x; \alpha_1, \alpha_3, \kappa, V_1) \mapsto \left(R, \lambda S, \lambda^{-1}x; \lambda^2\alpha_1, \lambda^2\alpha_3, \lambda\kappa, \lambda^2 V_1\right)\,, \tag{19}$$

$$(R, S, x; \alpha_1, \alpha_3, \kappa, V_1) \mapsto \left(\mu R, \mu S, x; \alpha_1, \mu^{-2}\alpha_3, \kappa, V_1\right). \tag{20}$$

The corresponding invariants for the Poincaré map are obtained by dropping the x components.

One can rescale (18) using these invariants to reduce to the cases where $\alpha_1 = 0\,, \pm 1$ and $\alpha_3 = 0\,, \pm 1$. We look in detail at the case $\alpha_1 = -1$, $\alpha_3 = -1$, corresponding to an attractive BEC with a negative chemical potential, where the underlying integrable system (with $V_1 = 0$) is a "figure eight" (consisting of a central saddle point and two exterior centers, as shown in figure 4c).

Because of the second rescaling (20), the parameter α_3 simply measures the size of phase space. The first rescaling (19) shows that decreasing κ increases the nonintegrable perturbation by a square law. Intuitively, a large lattice wave number κ implies that the Poincaré map corresponds to short-"time" integration in x and is thus "near" the vector field. With κ rescaled to 1, as was done in stating and proving our main result, the perturbation $V(x)$ in (18) has unit period.

Figures 1 – 3 show phase portraits of P at several amplitudes of the potential function for $(\alpha_1, \alpha_3, \kappa) = (-1, -1, 1)$. One obtains qualitatively similar results for other values of the lattice depth V_1 if the wave number κ is rescaled, as indicated above. As remarked previously, the phase space in these phase portraits is divided into two clearly distinct regions: an outer one in which the dynamics consists in

large measure of invariant circles and Cantor-like Aubry-Mather sets (that wind around the origin at large distance) and an inner one in which the dynamics is mostly chaotic. Our numerical simulations, which show the same scaling that our theoretical results indicate, suggest the presence of (parameter-dependent) integrable dynamics of positive but small measure inside the "chaotic sea."[36]

Remark 9 : A similar combination of islands of invariant tori within a chaotic sea occurs in the example of a parametrically forced planar pendulum.[5] The division of phase space into a most quasi-periodic and a mostly chaotic region is the typical behavior that one expects to observe in a large class of forced one *dof* Hamiltonian systems.[11]

Applying theorem 5 for $V(x)$ given by (17) implies that the system (18) has an invariant torus with frequency vector $(\omega, 1)$ provided ω satisfies the conditions of theorem 5. The R-amplitude is roughly equal to $R_{\max}$, given by

$$R_{\max} = 3b_1 \frac{\hbar\kappa\omega}{\pi\sqrt{-mg}}\,,$$

where $g < 0$ for the case of attractive BECs at hand [see equation (23) and lemma 11].

3.2 Example 2: BECs in Periodic Superlattices

Optical superlattices consist of small-scale lattices subjected to a long-scale periodic modulation. In recent experiments, BECs were created in superlattice potentials with a length scale (wave number) ratio of 1:3.[39] However, theoretical research concerning BECs in superlattices has thus far been sparse.[15,17,26,42]

To consider the case of (symmetric) periodic superlattices, we take the potential

$$V(x) = -\left[V_1\cos(\kappa_1 x) + V_2\cos(\kappa_2 x)\right]\,, \tag{21}$$

where $\kappa_2 > \kappa_1$ without loss of generality and $\kappa_2/\kappa_1 \in \mathbb{Q}$. The minimal period is $T = 2\pi/\kappa$, where $\kappa := \gcd(\kappa_1\,, \kappa_2)$.

Equation (7) is then written

$$\begin{aligned}
\frac{dR}{dx} &= S\,,\\
\frac{dS}{dx} &= -\alpha_1 R + \alpha_3 R^3 + V_1 R\cos(\kappa_1 x) + V_2 R\cos(\kappa_2 x)\,,\\
\frac{dx}{dx} &= 1\,,
\end{aligned} \tag{22}$$

where all the parameters are again experimentally adjustable.

Applying theorem 5 for $V(x)$ given by (21) with $\kappa_2/\kappa_1 \in \mathbb{Q}$ (i.e., for periodic superlattices) implies that (22) has an invariant torus with frequency vector $(\omega, 1)$

provided ω satisfies the conditions of theorem 5. As in the lattice case, the R-amplitude is roughly equal to $R_{\max}$, where

$$R_{\max} = 3b_1 \frac{\hbar\kappa\omega}{\pi\sqrt{-mg}},$$

and we recall that $2\pi/\kappa$ is the period of $V(x)$ and $g < 0$ for attractive BECs.

Remark 10 : If κ_2/κ_1 is not rational, then the potential function V is not periodic. If κ_1 and κ_2 satisfy a Diophantine condition, then one can prove the existence of invariant tori at large distance from the origin.[23] We conjecture that it is possible to quantify this existence result analogous to the periodic case.[11] If κ_1 and κ_2 are not Diophantine—for example if κ_2/κ_1 is a Liouville number—then one expects unbounded solutions and no invariant tori.[22]

4 Proof of the main result

To prove Theorem 5, we first construct action-angle coordinates explicitly. Then the KAM theorem of Chow et al.[11] will be employed to complete the proof after a suitable transformation of the action variable.

4.1 The action and K_0

Define the action by

$$I(h) = \int_{H_0=h} S\,\mathrm{d}R = 4\int_0^{R_{\max}} \sqrt{2h - 2z_4R^4}\,\mathrm{d}R,$$

where $H_0(R,S) = \frac{1}{2}S^2 + z_4R^4$ and $R_{\max} = R_{\max}(h) > 0$ is the solution of $H_0(R_{\max}, 0) = h$; that is, $R_{\max} = z_4^{-1/4}h^{1/4}$. With the substitution $u = R/R_{\max}$ and the relation $h = z_4R_{\max}^4$, the above integral reduces to

$$I(h) = 4\sqrt{2}b_1 z_4^{1/2} R_{\max}^3 = 4\sqrt{2}b_1 z_4^{-1/4} h^{3/4}. \tag{23}$$

Lemma 11 *The unperturbed Hamiltonian in action-angle coordinates is given by*

$$K_0(I) = 2^{-10/3} b_1^{-4/3} z_4^{1/3} I^{4/3}.$$

The proof follows from the calculation above, noting that the unperturbed Hamiltonian K_0 is the inverse of the function I [because $H_0(R,S) = K_0(I)$ for $I = I(H_0(R,S))$]. The function I is invertible, as

$$\frac{\partial I}{\partial h} = 3\sqrt{2}b_1 z_4^{-1/4} h^{-1/4} > 0.$$

Remark 12 : One could also define the action to be the area enclosed by the curve $\frac{1}{2}S^2 + \bar{z}_2 R^2 + z_4 R^4 = h$, where $\bar{z}_2$ is the average of z_2, or even the area enclosed by $H = h$ where ξ is considered as a parameter (i.e., $\xi' = 0$ in the unperturbed system). In the latter case the action and angle will depend on ξ. Although these two approaches leave a smaller term in the perturbation than our choice, and are therefore theoretically more pleasing, they lead to technical difficulties in the estimates we need to perform as the expressions for the action and angle will involve elliptic integrals that depend on the phase variables.

4.2 The angle

In the upper half plane ($S \geq 0$), we define the angle by

$$\phi(h,R) = \left(\frac{\partial I}{\partial h}\right)^{-1} \int_0^R \frac{1}{\bar{S}(h,w)}\,\mathrm{d}w \pmod 1,$$

where $\bar{S}(h,R) = \sqrt{2h - 2z_4R^4}$ is the positive solution of $H_0(R, \bar{S}(h,R)) = h$. Note that $\frac{\partial I}{\partial h} = \oint_{H_0=h} S^{-1}\,\mathrm{d}R$. A similar definition holds in the lower half plane, where $\phi = \frac{1}{2} - (\frac{\partial I}{\partial h})^{-1} \int_0^R \bar{S}^{-1}\,\mathrm{d}w \pmod 1$. From here on, we restrict to the upper half plane without loss of generality.

Lemma 13

$$\begin{aligned} \phi(h,R) &= \frac{1}{6b_1}\int_0^{R/R_{\max}} (1-u^4)^{-1/2}\,\mathrm{d}u \\ \bar{S}(h,R)\frac{\partial \phi}{\partial h}(h,R) &= -\frac{\sqrt{2}}{24b_1} h^{-1/2}\frac{R}{R_{\max}}. \end{aligned}$$

Defining $r = r(h,R) = R/R_{\max}(h)$, the lemma shows that ϕ depends only on r:

$$\phi(h,R) = \bar{\phi}(r(h,R)), \text{ where } \bar{\phi}(r) = \frac{1}{6b_1}\int_0^r (1-u^4)^{-1/2}\,\mathrm{d}u.$$

In particular, $\bar{\phi}(1) = 1/4$.

Proof: Using the definition of ϕ and the substitution $w = R_{\max}u$, we obtain

$$\begin{aligned} \phi &= \left(\frac{\partial I}{\partial h}\right)^{-1} \frac{1}{\sqrt{2}} z_4^{-1/2} R_{\max}^{-1} \int_0^r (1-u^4)^{-1/2}\,\mathrm{d}u \\ &= \frac{1}{6b_1} z_4^{-1/4} h^{1/4} R_{\max}^{-1} \int_0^r (1-u^4)^{-1/2}\,\mathrm{d}u, \end{aligned}$$

which proves the first formula. Furthermore,

$$\begin{aligned}\bar{S}(h,R)\frac{\partial\phi}{\partial h} &= -(2h-2z_4R^4)^{1/2}\frac{1}{6b_1}(1-r^4)^{-1/2}RR_{\max}^{-2}\frac{\partial R_{\max}}{\partial h}\\ &= -\frac{\sqrt{2h}}{24b_1}R_{\max}^{-1}z_4^{-1/4}h^{-3/4}r\\ &= -\frac{\sqrt{2}}{24b_1}h^{-1/2}r.\end{aligned}$$

□

4.3 Localization and rescaling

The system corresponding to K can be computed directly and is given by

$$\begin{aligned}\phi' &= K_0'(I)+f_1(\phi,I,\xi)\\ I' &= f_2(\phi,I,\xi)\\ \xi' &= 1\,,\end{aligned}$$

where $f_1(\phi,I,\xi)=-S\frac{\partial\phi}{\partial h}\frac{\partial H_1}{\partial R}$ and $f_2(\phi,I,\xi)=-S\frac{\partial I}{\partial h}\frac{\partial H_1}{\partial R}$.

For a fixed I_0, we define a localization transformation $(\phi,I,\xi)\mapsto(\phi,J,\xi)$ by $I=I_0+\beta(I_0)J$, with $\beta(I_0)=b_2I_0(\log(z_4I_0))^{-1}$, where $b_2\in\mathbb{R}_{>0}$ will be determined later. This takes the unperturbed torus $I=I_0$ to $J=0$ and rescales the action variable, so that the components f_1, f_2 of the perturbation are roughly the same size after rescaling and some other conditions are met (see remark 19 below). Although it is not a symplectic transformation, it nonetheless maps Hamiltonian systems to Hamiltonian systems.

Define $\omega=K_0'(I_0)$ and $m=\beta(I_0)K_0''(I_0)$, so that

$$\omega = \frac{1}{3}\cdot 2^{-4/3}b_1^{-4/3}z_4^{1/3}I_0^{1/3} \tag{24}$$

$$m = \frac{1}{9}\cdot 2^{-4/3}b_1^{-4/3}b_2\frac{z_4^{1/3}I_0^{1/3}}{\log(z_4I_0)}\,. \tag{25}$$

Lemma 14 *In (ϕ,J,ξ) coordinates, the system is written*

$$\phi'=\omega+mJ+g(J)+F_1(\phi,J,\xi)\ ,\ J'=F_2(\phi,J,\xi)\ ,\ \xi'=1,$$

where, for some $J_*, J^* \in (0, J)$,

$$\begin{aligned}
g(J) &= \frac{1}{2}\beta(I_0)^2 K_0'''(I_0 + \beta(I_0)J_*)J^2 \\
&= -\frac{1}{27}\cdot 2^{-4/3} b_1^{-4/3} z_4^{1/3} I_0^{1/3} \left(1 + \frac{b_2 J_*}{\log(z_4 I_0)}\right)^{-5/3} \left(\frac{b_2 J}{\log(z_4 I_0)}\right)^2 , \\
\frac{\partial g}{\partial J}(J) &= \beta(I_0)^2 K_0'''(I_0 + \beta(I_0)J^*)J \\
&= -\frac{1}{27}\cdot 2^{-1/3} b_1^{-4/3} b_2 \frac{z_4^{1/3} I_0^{1/3}}{\log(z_4 I_0)} \left(1 + \frac{b_2 J^*}{\log(z_4 I_0)}\right)^{-5/3} \frac{b_2 J}{\log(z_4 I_0)} , \\
F_1(\phi, J, \xi) &= f_1(\phi, I_0 + \beta(I_0)J, \xi) \\
&= \frac{1}{3}\cdot 2^{-2/3} b_1^{-2/3} z_2(\xi) r^2 z_4^{-1/3} I_0^{-1/3} \left(1 + \frac{b_2 J}{\log(z_4 I_0)}\right)^{-1/3} , \\
F_2(\phi, J, \xi) &= \beta(I_0)^{-1} f_2(\phi, I_0 + \beta(I_0)J, \xi) \\
&= -3\cdot 2^{1/3} b_1^{1/3} z_2(\xi) r (1 - r^4)^{1/2} b_2^{-1} \frac{\log(z_4 I_0)}{z_4^{1/3} I_0^{1/3}} \left(1 + \frac{b_2 J}{\log(z_4 I_0)}\right)^{2/3} .
\end{aligned}$$

The lemma shows that the nonintegrable parts F_1 and F_2 are order $I_0^{-1/3}$ in leading term; this would have been order 1 in case the original potential U had had a cubic term.

Proof: Write $\Omega(J) = K_0'(I_0 + \beta(I_0)J)$, so that $\omega = \Omega(0)$ and $m = \Omega'(0)$. By Taylor's theorem,

$$g(J) = \Omega(J) - \omega - mJ = \frac{1}{2}\Omega''(J_*)J^2 \ , \ g'(J) = \Omega'(J) - m = \Omega''(J^*)J \, .$$

Furthermore, $\beta(I_0)J' = I'$. The expressions for g, g', F_1, and F_2 follow by direct calculation from (23) and lemma 13.

□

4.4 Proof of Theorem 5

The rescaled system is a perturbation of $\phi' = \omega + mJ + g(J)$, $J' = 0$. The unperturbed system has an invariant torus $J = 0$ with ϕ-frequency ω. Assume that ω is of constant type with parameter $\gamma > 0$. We now study the persistence of this torus under the perturbation $F = (F_1, F_2)$.

For $d > 0$, $\eta = 18\gamma$, and $\rho = (3m)^{-1}\eta$ we define a (complex) neighborhood $\mathcal{D}_0$ of the unperturbed torus by

$$\mathcal{D}_0 = \mathcal{D}_0(\eta, \rho, d) = \{(\phi, J, \xi) \in \mathbb{C}/\mathbb{Z} \times \mathbb{C} \times \mathbb{R}/\mathbb{Z} : |\mathrm{Im}(\phi)| \le \eta, |J| < \rho\} + 2d \, .$$

The KAM theorem of Chow et al.[11] now shows that the perturbed system has an invariant torus with frequency ω, satisfying $|J| \leq \frac{11}{19}d + \rho$, provided

$$\begin{aligned} ||\frac{\partial g}{\partial J}||_{\mathcal{D}_0} &< m/4\,, \qquad (26) \\ \omega_0 &\leq \omega\,. \qquad (27) \end{aligned}$$

The first of these conditions is a twist condition, and the second states that the perturbation is small enough, where ω_0 is defined as follows. Let $c = 5.04$, and $||F||_{\mathcal{D}_0} = \max\{||F_1||_{\mathcal{D}_0}, ||F_2||_{\mathcal{D}_0}\}$. Let L_W denote the Lambert W function (i.e., the inverse of $W \mapsto We^W$). Then,

$$\begin{aligned} \omega_0 &= \alpha_0 \max\left\{1, \frac{1}{\log 2} L_W(b \log 2)\right\}\,, \\ b &= \frac{2+3m}{c\gamma^2} \max\left\{12, \frac{7^8}{108(\eta - 6\gamma)^4}\right\} \max\{md, 2||F||_{\mathcal{D}_0}\}\,, \qquad (28) \\ \alpha_0 &= \frac{3 + 12(\eta + 2d)}{2d}\left(||F||_{\mathcal{D}_0} + 2C \max\left\{1, \frac{2||F||_{\mathcal{D}_0}}{md}\right\}\right)\,, \\ C &= \frac{2}{3}\max\{m(2d+\rho) + ||g||_{\mathcal{D}_0} + ||F||_{\mathcal{D}_0}, 1\}\,. \end{aligned}$$

Lemma's 15 – 18 show that the twist and smallness conditions follow from conditions (11) – (16) of Theorem 5.

Lemma 15 *Condition (26) follows from (13).*

Proof: For $|J| \leq \rho + 2d$, it follows that

$$\left|\left|\frac{b_2 J}{\log(M)}\right|\right|_{\mathcal{D}_0} \leq b_2 \frac{\rho + 2d}{\log(M)} = L \leq \frac{47}{200}\,.$$

Hence, for J^* as in lemma 14,

$$\left|\left|\left(1 + \frac{b_2 J^*}{\log(M)}\right)^{-5/3} \frac{b_2 J}{\log(M)}\right|\right|_{\mathcal{D}_0} \leq \left(1 - \frac{47}{200}\right)^{-5/3} \frac{47}{200} < \frac{3}{8}\,.$$

The desired result now follows from lemma 14.

□

Lemma 16 *Let $r = R/R_{\max}$ as before. Then,*

$$\begin{aligned} ||r||_{\mathcal{D}_0} &\leq 1 + 24 b_1(\eta + 2d) \\ ||r(1-r^4)^{1/2}||_{\mathcal{D}_0} &\leq [1 + 24 b_1(\eta + 2d)]^3. \end{aligned}$$

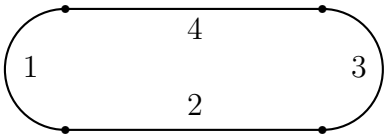

Figure 6: The set $\mathcal{E}$, with labels for the four parts of its boundary (two semi-circles and two line segments).

Proof: Without loss of generality, we restrict to ϕ with $\mathrm{Re}(\phi) \in [0, \frac{1}{4}]$ (mod 1). Observe that $|\mathrm{Im}\phi| \leq \eta + 2d$ in $\mathcal{D}_0$. Thus, we can consider $\phi \in \bar{\mathcal{D}} = \{\phi \in \mathbb{C}/\mathbb{Z} : \mathrm{Re}(\phi) \in [0, \frac{1}{4}](\mathrm{mod}\ 1), |\mathrm{Im}\phi| \leq \eta + 2d\}$.

Let $\mathcal{E}(\varepsilon) = [0,1] + \varepsilon \subset \mathbb{C}$. It is obvious that r will be in $\mathcal{E}$ for large enough ε. Let ε be the smallest number such that $r = r(\phi) \in \mathcal{E} = \mathcal{E}(\varepsilon)$ for all $\phi \in \bar{\mathcal{D}}$. Hence, there exists a $\phi_0 \in \bar{\mathcal{D}}$ such that $r(\phi_0)$ is on the boundary of $\mathcal{E}$. Furthermore, $r(\mathrm{Re}(\phi_0)) \in [0,1]$. Therefore, by the mean value theorem,

$$\varepsilon \leq |r(\phi_0) - r(\mathrm{Re}(\phi_0))| \leq \left|\left|\frac{\partial r}{\partial \phi}\right|\right|_{\bar{\mathcal{D}}} (\eta + 2d)\,.$$

By definition, $\frac{\partial \phi}{\partial r}(r) = (6b_1)^{-1}(1-r^4)^{-1/2}$. Thus,

$$\frac{\partial r}{\partial \phi}(\phi) = 6b_1(1-r^4)^{1/2}\,.$$

We will now show that $||1-r^4||_{\mathcal{E}} \leq (1+\varepsilon)^4$. By the maximum modulus theorem, $||1-r^4||_{\mathcal{E}}$ is attained on the boundary of $\mathcal{E}$, which looks like a stadium and consists of four parts (see figure 6). Part 1 is parametrized by $r = \varepsilon\exp(i\theta)$, where $\theta \in [\pi/2, 3\pi/2]$. Hence, $|1-r^4| \leq 1+\varepsilon^4 \leq (1+\varepsilon)^4$. Part 2 is parametrized by $r = u - \varepsilon i$, with $u \in [0,1]$. Consequently, $|1-r^4| \leq 1 - u^4 + 4u^3\varepsilon + 6u^2\varepsilon^2 + 4u\varepsilon^3 + \varepsilon^4 \leq 1 + 4\varepsilon + 6\varepsilon^2 + 4\varepsilon^3 + \varepsilon^4 \leq (1+\varepsilon)^4$. Part 3 is parametrized by $r = 1 + \varepsilon\exp(i\theta)$, where $\theta \in [-\pi/2, \pi/2]$. Hence, $|1-r^4| \leq 4\varepsilon + 6\varepsilon^2 + 4\varepsilon^3 + \varepsilon^4 \leq (1+\varepsilon)^4$. Part 4 is similar to part 2.

Thus, we have found that

$$\varepsilon \leq 6b_1||1-r^4||_{\mathcal{E}}^{1/2}(\eta + 2d) \leq 6b_1(\eta+2d)(1+\varepsilon)^2\,.$$

A straightforward calculation with this result then shows that $\varepsilon \leq 24b_1(\eta + 2d)$, which implies the first statement of the lemma. To prove the second statement, we use the fact that $||1-r^4||_{\mathcal{D}_0}^{1/2} \leq (1+\varepsilon)^2 \leq [1 + 24b_1(\eta+2d)]^2$, as already shown.

□

Lemma 17 *Assume that (12), (13), (14), and (16) hold. Then,*

$$||g||_{\mathcal{D}_0} \leq \frac{2^{-4/3}}{27} b_1^{-4/3}(1-L)^{-5/3}L^2M^{1/3}\,, \tag{29}$$

$$||F||_{\mathcal{D}_0} \leq \nu d b_1^{-4/3} b_2 \frac{M^{1/3}}{\log(M)}\,. \tag{30}$$

Proof: The assumption on M implies that $\log M > 0$. As in the proof of lemma 15, $\left|\left|\frac{b_2 J}{\log(M)}\right|\right|_{\mathcal{D}_0} \leq L < 1$, and the result then follows from lemma 14 and lemma 16. Condition (14) implies that $||F_1||_{\mathcal{D}_0} \leq ||F_2||_{\mathcal{D}_0}$, and (16) bounds $||z_2||_{\mathcal{D}_0}$.

□

Lemma 18 *Assume that* $\nu \leq \frac{1}{9} \cdot 2^{-7/3}$ *and* $\gamma = \eta/18 \leq \frac{49}{72}$ *as in Theorem 5. If conditions (12) – (16) hold, then*

$$\omega_0 \leq \frac{A}{\log(2)} \left(\frac{1}{3} + \frac{\log(B)}{\log(M)} \right) M^{1/3}.$$

Theorem 5 now follows immediately from this lemma and the expression for $\omega = K'(I_0)$.

Proof: By the previous lemma,

$$C \leq \frac{2}{3} \max \left\{ \frac{\eta}{3} + \left(\frac{2^{-1/3}}{9} + \nu \right) d b_1^{-4/3} b_2 \frac{M^{1/3}}{\log(M)} + \frac{2^{-4/3}}{27} b_1^{-4/3} (1-L)^{-5/3} L^2 M^{1/3}, 1 \right\}.$$

A straightforward calculation shows that $\nu \leq \frac{1}{9} \cdot 2^{-7/3}$ implies $2||F||_{\mathcal{D}_0} \leq md$. Hence,

$$\begin{aligned}
\alpha_0 &= \frac{3 + 12(\eta + 2d)}{2d} (||F||_{\mathcal{D}_0} + 2C) \\
&\leq \frac{1 + 4(\eta + 2d)}{d} \max \left\{ \frac{2\eta}{3} M^{-1/3} \log(M) + \left(\frac{2^{2/3}}{9} + \frac{7\nu}{2} \right) d b_1^{-4/3} b_2 + \right. \\
&\quad \left. \frac{2^{-1/3}}{27} b_1^{-4/3} (1-L)^{-5/3} L^2 \log(M), 2M^{-1/3} log(M) + \frac{3\nu}{2} d b_1^{-4/3} b_2 \right\} \frac{M^{1/3}}{\log(M)} \\
&= A \frac{M^{1/3}}{\log(M)}.
\end{aligned}$$

From $\gamma = \eta/18 \leq 49/72$, it follows that $12 \leq \frac{1}{108} 7^8 (\eta - 6\gamma)^{-4}$. We observe that γ does not appear in any other quantity except for b. The choice $\gamma = \eta/18$ minimizes b. We obtain

$$\begin{aligned}
b &= \frac{7^8 \cdot 18^2 \cdot 3^4 (2 + 3m)}{108 \cdot 2^4 c \eta^6} md \\
&= 2^{-4} \cdot 3^5 \cdot 7^8 c^{-1} \eta^{-6} (2 + 3m) md \\
&= 2^{-13/3} \cdot 3^3 \cdot 7^8 c^{-1} d b_1^{-4/3} b_2 \eta^{-6} \left(\frac{1}{\log(M)} + \frac{2^{-7/3}}{3} b_1^{-4/3} b_2 \frac{M^{1/3}}{\log^2(M)} \right) M^{1/3} \\
&= B M^{1/3}.
\end{aligned}$$

From $b \geq 2$, we see that $L_W(b \log(2)) \leq \log(b)$. The result follows.

□

Remark 19 : The transformation $I \mapsto J$ is chosen such that ω and ω_0 have the same growth rate in I_0 and z_4 (i.e., in the leading term). Independent of the rescaling, ω grows as $I_0^{1/3}$. On the other hand, $\omega_0 \leq \alpha_0 \log(b)/\log(2)$ (if $b \geq 2$). Because b grows as some power of I_0, it follows that α_0 must grow as $I_0^{1/3}/\log(I_0)$. Analysis of the dependence on z_4 then leads to the chosen rescaling.

Acknowledgements

We are grateful to Peter Engels, Panos Kevrekidis, Boris Malomed, Alexandru Nicolin, and Li You for useful discussions concerning this research. MAP was supported by a VIGRE grant awarded to the School of Mathematics at Georgia Tech. MvN was partially supported by the Center for Dynamical Systems and Nonlinear Studies at Georgia Tech and partially by EPSRC grant GR/S97965/01. YY was partially supported by NSF grant DMS0204119.

References

[1] B. P. Anderson and M. A. Kasevich. Macroscopic quantum interference from atomic tunnel arrays. *Science*, 282(5394):1686–1689, November 1998.

[2] M. H. Anderson, J. R. Ensher, M. R. Matthews, C. E. Wieman, and E. A. Cornell. Observation of Bose-Einstein condensation in a dilute atomic vapor. *Science*, 269(5221):198–201, July 1995.

[3] V. I. Arnol'd. Small denominators and problems of stability of motion in classical and celestial mechanics. *Uspehi Mat. Nauk*, 18(6 (114)):91–192, 1963. translated in Russian Math. Surveys.

[4] S. Aubry and P. Y. Le Daeron. The discrete Frenkel-Kontorova model and its extensions. I. Exact results for the ground-states. *Phys. D*, 8(3):381–422, 1983.

[5] H.W. Broer, I. Hoveijn, M. van Noort, C. Simó, and G. Vegter. The parametrically forced pendulum: a case study in $1\frac{1}{2}$ degree of freedom. *J. Dynam. Differential Equations*, 16(4):897 – 947, 2004.

[6] H.W. Broer, M. van Noort, and C. Simó. Existence and measure of 2-quasiperiodicity in Hamiltonian one-and-a-half degree of freedom systems. In *Equadiff - International conference on Differential Equations, Hasselt 2003*, pages 595 – 600. World Scientific, 2005.

[7] Jared C. Bronski, Lincoln D. Carr, Bernard Deconinck, and J. Nathan Kutz. Bose-Einstein condensates in standing waves: The cubic nonlinear Schrödinger equation with a periodic potential. *Physical Review Letters*, 86(8):1402–1405, February 2001.

[8] R. Carretero-González and K. Promislow. Localized breathing oscillations of Bose-Einstein condensates in periodic traps. *Physical Review A*, 66(033610), September 2002.

[9] F. S. Cataliotti, L. Fallani, F. Ferlaino, C. Fort, P. Maddaloni, and M. Inguscio. Superfluid current disruption in a chain of weakly coupled Bose-Einstein condensates. *New Journal of Physics*, 5:71.1–71.7, June 2003.

[10] Guishi Chong, Wenhua Hai, and Qiongtao Xie. Spatial chaos of trapped Bose-Einstein condensate in one-dimensional weak optical lattice potential. *Chaos*, 14(2):217–223, June 2004.

[11] S.-N. Chow, M. van Noort, and Y. Yi. Quasiperiodic dynamics in Hamiltonian $1\frac{1}{2}$ degree of freedom systems far from integrability. *J. Diff. Eq.*, 212(2):366–393, 2005.

[12] Franco Dalfovo, Stefano Giorgini, Lev P. Pitaevskii, and Sandro Stringari. Theory of Bose-Einstein condensation on trapped gases. *Reviews of Modern Physics*, 71(3):463–512, April 1999.

[13] K. B. Davis, M.-O. Mewes, M. R. Andrews, N. J. van Druten, D. S. Durfee, D. M. Kurn, and W. Ketterle. Bose-Einstein condensation in a gas of sodium atoms. *Physical Review Letters*, 75(22):3969–3973, November 1995.

[14] R. Dieckerhoff and E. Zehnder. Boundedness of solutions via the twist-theorem. *Ann. Scuola Norm. Sup. Pisa Cl. Sci. (4)*, 14(1):79–95, 1987.

[15] L. A. Dmitrieva and Yu. A. Kuperin. Spectral modelling of quantum superlattice and application to the Mott-Peierls simulated transitions. arXiv:cond-mat/0311468, November 19 2003.

[16] Elizabeth A. Donley, Neil R. Claussen, Simon L. Cornish, Jacob L. Roberts, Eric A. Cornell, and Carl E. Weiman. Dynamics of collapsing and exploding Bose-Einstein condensates. *Nature*, 412:295–299, July 19th 2001.

[17] Y. Eksioglu, P. Vignolo, and M.P. Tosi. Matter-wave interferometry in periodic and quasi-periodic arrays. arXiv:cond-mat/0404458, April 2004.

[18] Markus Greiner, Olaf Mandel, Tilman Esslinger, Theodor Hänsch, and Immanuel Bloch. Quantum phase transition from a superfluid to a Mott insulator in a gas of ultracold atoms. *Nature*, 415(6867):39–44, January 3, 2002.

[19] E. W. Hagley, L. Deng, M. Kozuma, J. Wen, K. Helmerson, S. L. Rolston, and W. D. Phillips. A well-collimated quasi-continuous atom laser. *Science*, 283(5408):1706–1709, March 1999.

[20] M.R. Herman. *Sur les courbes invariantes par les difféomorphismes de l'anneau, vol. 1*, volume 103-104 of *Astérisque*. Société Mathématique de France, 1983.

[21] M.R. Herman. *Sur les courbes invariantes par les difféomorphismes de l'anneau, vol. 2*, volume 144 of *Astérisque*. Société Mathématique de France, 1986.

[22] H. Huang. Destruction of invariant tori in pendulum-type equations. *J. Diff. Eq.*, 146(1):67–89, 1998.

[23] M. Levi and E. Zehnder. Boundedness of solutions for quasiperiodic potentials. *SIAM J. Math. Anal.*, 26(5):1233 – 1256, 1995.

[24] J. E. Littlewood. Unbounded solutions of an equation $\ddot{y} + g(y) = p(t)$, with $p(t)$ periodic and bounded, and $g(y)/y \to \infty$ as $y \to \pm\infty$. *J. London Math. Soc.*, 41:491–507, 1966.

[25] B. Liu. Boundedness for solutions of nonlinear Hill's equations with periodic forcing terms via Moser's twist theorem. *J. Differential Equations*, 79(2):304–315, 1989.

[26] Pearl J. Y. Louis, Elena A. Ostrovskaya, and Yuri S. Kivshar. Matter-wave dark solitons in optical lattices. *Journal of Optics B: Quantum and Semiclassical Optics*, 6:S309–S317, 2004.

[27] Pearl J. Y. Louis, Elena A. Ostrovskaya, Craig M. Savage, and Yuri S. Kivshar. Bose-Einstein condensates in optical lattices: Band-gap structure and solitons. *Physical Review A*, 67(013602), 2003.

[28] M. Machholm, A. Nicolin, C. J. Pethick, and H. Smith. Spatial period-doubling in Bose-Einstein condensates in an optical lattice. *Physical Review A*, 69(043604), 2004.

[29] John N. Mather. Existence of quasiperiodic orbits for twist homeomorphisms of the annulus. *Topology*, 21(4):457–467, 1982.

[30] C. Menotti, A. Smerzi, and A. Trombettoni. Superfluid dynamics of a Bose-Einstein condensate in a periodic potential. *New Journal of Physics*, 5(112):112.1–112.20, September 2003.

[31] O. Morsch, J. H. Müller, M. Christiani, D. Ciampini, and E. Arimondo. Bloch oscillations and mean-field effects of Bose-Einstein condensates in 1D optical lattices. *Physical Review Letters*, 87(140402), September 2001.

[32] J. Moser. Recent developments in the theory of Hamiltonian systems. *SIAM Rev.*, 28(4):459–485, 1986.

[33] J. Moser. Minimal foliations on a torus. In M. Giaquinta, editor, *Topics in calculus of variations (Montecatini Terme, 1987)*, volume 1365 of *Lecture Notes in Mathematics*, pages 62–99. Springer-Verlag, 1989.

[34] J. Moser. Quasi-periodic solutions of nonlinear elliptic partial differential equations. *Bol. Soc. Brasil. Mat. (N.S.)*, 20(1):29–45, 1989.

[35] A.I. Neishtadt. Estimates in the Kolmogorov theorem on conservation of conditionally periodic motions. *J. Appl. Math. Mech.*, 45(6):1016–1025, 1981.

[36] A.I. Neishtadt, V.V. Sidorenko, and D.V. Treschev. Stable periodic motions in the problem on passage through a separatrix. *Chaos*, 7(1):2–11, 1997.

[37] C. Orzel, A. K. Tuchman, M. L. Fenselau, M. Yasuda, and M. A. Kasevich. Squeezed states in a Bose-Einstein condensate. *Science*, 291(5512):2386, March 2001.

[38] P. Pedri, L. Pitaevskii, S. Stringari, C. Fort, S. Burger, F. S. Cataliotii, P. Maddaloni, F. Minardi, and M. Inguscio. Expansion of a coherent array of Bose-Einstein condensates. *Physical Review Letters*, 87(22):220401, November 2001.

[39] S. Peil, J. V. Porto, B. Laburthe Tolra, J. M. Obrecht, B. E. King, M. Subbotin, S. L. Rolston, and W. D. Phillips. Patterned loading of a Bose-Einstein condensate into an optical lattice. *Physical Review A*, 67(051603(R)), 2003.

[40] Mason A. Porter and Predrag Cvitanović. Modulated amplitude waves in Bose-Einstein condensates. *Physical Review E*, 69(047201), 2004.

[41] Mason A. Porter and Predrag Cvitanović. A perturbative analysis of modulated amplitude waves in Bose-Einstein condensates. *Chaos*, 14(3):739–755, September 2004.

[42] Mason A. Porter and P. G. Kevrekidis. Bose-Einstein condensates in superlattices. *SIAM Journal of Applied Dynamical Systems*, To appear (arXiv/nlin.PS/0406063), 2005.

[43] J. V. Porto, S. Rolston, B. Laburthe Tolra, C. J. Williams, and W. D. Phillips. Quantum information with neutral atoms as qubits. *Philosophical Transactions: Mathematical, Physical & Engineering Sciences*, 361(1808):1417–1427, July 2003.

[44] A. Smerzi, A. Trombettoni, P. G. Kevrekidis, and A. R. Bishop. Dynamical superfluid-insulator transition in a chain of weakly coupled Bose-Einstein condensates. *Physical Review Letters*, 89:170402, 2002.

[45] Quentin Thommen, Jean Claude Garreau, and Véronique Zehnlé. Classical chaos with Bose-Einstein condensates in tilted optical lattices. *Physical Review Letters*, 91:210405, November 2003.

[46] K. G. H. Vollbrecht, E. Solano, and J. L. Cirac. Ensemble quantum computation with atoms in periodic potentials. *Physical Review Letters*, 93(220502), 2004.

[47] Biao Wu, Roberto B. Diener, and Qian Niu. Bloch waves and Bloch bands of Bose-Einstein condensates in optical lattices. *Physical Review A*, 65(025601), 2002.

[48] J. You. Invariant tori and Lagrange stability of pendulum-type equations. *J. Diff. Eq.*, 85:54 – 65, 1990.